

Opo: A Wearable Sensor for Capturing High-Fidelity Face-to-Face Interactions

William Huang, Ye-Sheng Kuo, Pat Pannuto, Prabal Dutta

Electrical Engineering and Computer Science Department

University of Michigan

Ann Arbor, MI 48109

{wwhuang,samkuo,ppannuto,prabal}@umich.edu

Abstract

Currently, researchers study face-to-face interactions using wearable sensors and smartphones which provide 2 to 5 m proximity sensing every 20 to 300 s. However, studying interaction distance, which is known to impact disease spread, communication behavior, and other phenomenon, has proven challenging. Smartphones are limited by their inaccurate and/or impractical ranging capabilities, while wearable sensors are limited by their need for infrastructure nodes, bulkiness, and/or inaccurate ranging. To address these challenges, we present Opo, a 14 cm², 11.4 g “lapel pin” built from commercial components. Opo sensors range neighbors every 2 s up to 2 m away with 5% average error, all while requiring zero infrastructure and improving upon current wearable sensors’ accuracy and power usage. The cornerstone of Opo is an ultrasonic wakeup circuit that draws 19 µA when no neighbors are present. This enables Opo sensors to discover and range neighbors without the need for infrastructure nodes and slow or power-hungry RF discovery protocols. Thus, Opo is able to sense interaction distance with high accuracy (5 cm) and temporal fidelity (2 s) on a limited power budget.

Categories and Subject Descriptors

B.4.1 [HARDWARE]: Input/Output and Data Communications—*Data Communications Devices*

General Terms

Design, Experimentation, Human Factors, Measurement
Keywords

Ranging, Ultrasonic, RF, Time of Flight, Low-Power

Permission to make digital or hard copies of part or all of this work for personal or classroom use is granted without fee provided that copies are not made or distributed for profit or commercial advantage and that copies bear this notice and the full citation on the first page. Copyrights for third-party components of this work must be honored. For all other uses, contact the Owner/Author.

Copyright is held by the owner/author(s).

Sensys'14, November 3–5, 2014, Memphis, TN, USA.
ACM 978-1-4503-3143-2/14/11.
<http://dx.doi.org/10.1145/2668332.2668338>

1 Introduction

Face-to-face interactions are a crucial part of our lives, and the interaction distance at which they occur is important in a variety of psychological [20], cultural [12], and epidemiological [48] areas. Case studies have shown that interaction distance informs and affects various psychological elements, cultural norms, and personal behaviors. For example, interaction distance affects stress levels [20], reflects racial attitudes [34], and informs communication behavior [55] and inter-cultural differences [12, 57]. In addition, case studies have shown that interaction distance influences influenza infection rates [3, 48, 61]. Looking to the future, interaction distance may influence human robotic interaction usability, motion planning, and navigation [58, 59].

Traditionally, face-to-face interactions are studied via surveys and other forms of self reporting. However, their burden on users, subjectivity, and coarse-grained resolution have driven researchers to develop more objective and fine-grained interaction sensing systems. Currently, the two most popular solutions are Bluetooth scanning smartphones [10] and wearable RF/RSSI scanning sensors [21].

Smartphone deployments use Bluetooth scans to determine if two people are within 5 m of each other every 5 minutes [10, 30]. Smartphones are also able to provide contextual interaction information such as GPS location, and have seen steadily increasing market penetration [6]. However, in addition to their limited ranging capabilities, Bluetooth scans give no indication of user orientation, which can be a critical factor in fields such as epidemiology [19, 60]. Furthermore, while smartphone penetration as a whole has been steadily increasing, it is unclear when the platform will become truly universal. Smartphone penetration varies significantly between age group, education level, community type, and household income [4, 5]. For example, only 37% of U.S teens own smartphones [7], and only 47-53% of households with incomes of \$50,000 or less own smartphones [5]. In addition, the multitude of software and hardware platforms complicate support and sensor calibration. In practice, researchers commonly buy smartphones for interaction sensing deployments, giving them a standardized hardware and software platform [9, 10, 18, 33]. These strengths and weaknesses result in smartphones typically being used for in-depth interaction studies of small groups of people.

Wearable sensors typically determine if users are near each other using the same principles as Bluetooth scans. They are less expensive than smartphones, offer better temporal fidelity, and tunable distance cutoffs. This has led to large scale deployments on the order of 1000s of participants with more fine-grained interaction data than smartphone deployments have provided [21, 50]. In most deployments, these systems are tuned to sense if participants are within 2 m of each other at a 20 s temporal fidelity [21, 50].

However, case studies have shown that more accurate interaction distance sensing could inform research in a variety of fields. For example, differences in interaction distance, rather than the binary within 2 m or 5 m proximity estimates that current systems provide, have been found to be significant in verbal communication [55], obesity stigmatism in children [47], stress [20], racial attitudes [34], and influenza spread [44, 61, 62]. Interaction distance is also thought to influence optimal robot navigation, usability, and motion planning in human robot interactions [58, 59]. In our survey of related works, we find a universal desire for sub-meter interaction distance accuracy, with studies indicating that there are still insights to be gained from higher accuracy in cultural, social, robotics, and epidemiological fields [14, 19, 57, 58].

Our survey of related work finds that only TDoA schemes reliably offer sub-meter accuracy in indoor environments. TDoA, or time-difference-of-arrival, schemes simultaneously send a beacon in a fast medium (RF) and a slow medium (audio or ultrasonic), and use the time difference of arrival at the receiver to estimate distance. TDoA smartphone and wearable sensor systems exist, but they all lack one key feature: usability. Smartphones are able to accurately sense distance when facing each other [41], but these orientation dependent systems fail in real-world situations where phones are in a pocket or purse. TDoA wearable sensor systems also exist, but require infrastructure nodes to operate, limiting their usability [22, 46]. Rather than being able to characterize a target population’s interactions, infrastructure dependent systems are limited to characterizing interactions in specific settings. Infrastructure-free wearable sensor systems have thus far only been able to sense proximity, rather than actually measure interaction distance.

To bridge the gap between usability and interaction distance sensing, we design and evaluate Opo, a infrastructure-free wearable sensor system that can measure face-to-face interaction distance with an average error of 5%. In addition, Opo improves upon the 20 s temporal resolution of current infrastructure-free wearable sensor systems by offering a 2 s temporal resolution while increasing power performance by an estimated 26x over state-of-the-art wearable sensors. Our key contribution is identifying the architectural and design choices necessary to enable unobtrusive and easily deployable wearable sensors for capturing face-to-face interactions and the distances at which they occur.

Our key insight is that we can combine ultrasonic/RF TDoA ranging and fast neighbor discovery while maintaining a high battery life via a novel ultrasonic (UL) wakeup frontend, which can be made from commercial parts. Our UL wakeup frontend draws 19 μ A when idle, allowing our wearable sensors to remain asleep until a neighbor appears

to wake it up, rather than constantly running an RF discovery protocol. Furthermore, Opo enables wearable sensors to synchronize and range in a *broadcast* fashion, synchronizing and ranging with all n neighbors per transmission. In contrast, most systems require all n neighbors to synchronize and range with one another, resulting in n^2 synchronizing/ranging events. Opo broadcast events cost 820 μ J, the cost of an ultrasonic pulse (35 μ J) and RF packet (785 μ J).

To evaluate Opo, we first conduct controlled tests on ranging error (2 cm) and angular offset sensitivity (only 6% error when two people are standing next to each other in a circle of six). Second, we use Opo to capture human interactions in a variety of settings (hallway conversations, short interactions, close encounters, speed dating, and group chats) with ground truth provided by hand measurements. We find that Opo performs well and captures all but 10% of the shortest (5 s) face-to-face interactions tested. Third, we evaluate Opo’s various subsystems’ energy costs to build an empirical energy model of Opo’s operation. Fourth, we perform a week long deployment with 8 participants to demonstrate real-world operation and the importance of infrastructure-free operation. Finally, we explore techniques to reduce angular offset errors, congestion, and power usage.

2 Background and Related Work

Surveys and self-reporting provide valuable information, but are highly subjective, coarse-grained, and laborious for users. These drawbacks have motivated researchers to explore more objective, fine-grained, and automated solutions to study face-to-face interactions [13, 19, 32]. Table 1 compares Opo to other localization/ranging systems.

2.1 Pure RF Techniques and Systems

Pure RF ranging techniques are appealing since an RF channel is often needed as a data link regardless of application. Several smartphone systems sense interactions by using Bluetooth scans to detect neighboring phones. Such systems can sense if two people are within 5 m of each other, but cannot accurately sense interaction distance beyond that [8, 9, 18, 64]. To conserve battery life, such systems typically provide 5 min temporal fidelity. Smartphone systems have typically been used to conduct in depth studies of small groups of people, leveraging GPS and other components to provide contextual interaction information.

Wearable sensor systems have used a similar technique, RF scanning, to sense face-to-face interactions in larger groups. OpenBeacon uses active RFID tags [15] worn like name badges; others use Irene [21], WREN [21], or TelosB [27] wireless sensors. These deployments have reported a cutoff proximity of 2 m at a 20 s temporal fidelity.

To complement raw proximity detection, some studies have used the received signal strength indicator (RSSI) reported by many radios to estimate range [15, 27]. However, the effective irradiated power from body-worn radios can be significantly different and much more dynamic than simple models would suggest, due to absorption, attenuation, reflection, and shadowing. Moreover, antenna beam forms tend not to be perfectly uniform, further introducing error into RSSI measurements. Even in relatively static conditions, RSSI ranging is only accurate to within 2 m [25, 38, 51].

System	Ranging Method	Ranging Accuracy	Infrastructure	Time Resolution	Size	Battery Size	Battery Life	Tested on People
WREN [21]	RF Scan	200 cm	No	20 s	13 cm ²	180 mAh	16 hr	Yes
TelosB [1, 50]	RSSI Sensing	200 cm	No	20 s	20 cm ²	4000 mAh ^a	16 hr	Yes
Social fMRI [9]	Bluetooth Scan	500 cm	No	300 s	N/A	N/A	N/A	Yes
WASP [52]	RF ToF	50 cm	Yes	.04 s	N/A	6.5 Ah	10 hr	Yes ^b
Cricket [46]	UL/RF TDoA	10 cm	Yes	1 s	40 cm ²	4000 mAh ^a	N/A	Yes
iBadge [40]	UL/RF TDoA	10 cm	Yes	N/A	38.5 cm ²	N/A	5 hr	Yes
RADAR [11]	RF Fingerprinting	2500 cm	Pseudo ^c	N/A	N/A	N/A	N/A	Yes
Dolphin [36]	UL ToF	24 cm ^d	Yes	13 s	N/A	N/A	N/A	No
Future UL [45]	UL AoA, ToA	sub-cm	Yes	1 s	N/A	N/A	N/A	No
Opo	UL/RF TDoA	5 cm	No	2 s	14 cm²	40 mAh	93 hr	Yes

^a Systems used 2x AA batteries. Listed mAh is average mAh of two alkaline AA batteries.

^b WASP evaluated humans in outdoor settings, but not indoor environments.

^c RADAR assumes access to a pre-existing wireless network, ability to build and access an RF map of a building.

^d DOLPHIN accuracy under semi-ideal, static conditions. Under ideal conditions, accuracy is 2 cm

Table 1: Comparison of Opo to systems representing various ranging techniques. Opo is the only infrastructure-free system that can characterize interactions at a sub-meter level. Infrastructure-dependent systems offer high spatial fidelity, but are laborious, costly, and physically bounded, limiting usability. Pseudo-infrastructure systems assume pre-existing WiFi coverage, and require fingerprint mapping efforts, again limiting usability.

An improvement over RSSI measurement is coordinated pairwise RF time-of-flight (RF ToF) ranging, a peer-to-peer approach supported by systems such as Waldo [28] and WASP [52]. RF ToF works by measuring the round trip time (RTT) of a radio packet between two nodes. Unfortunately, measurement accuracy is heavily affected by multipath, which is prevalent in indoor environments [52]. In static conditions not involving humans, such systems are accurate to within 0.5 m 65% of the time [52].

In addition, pairwise RF ToF systems are power hungry due to the high-speed processing needed to range with sub-meter resolution, requiring up to 2.5 W for transmissions and 2 W for receptions [52]. Pairwise systems also scale poorly with study size, requiring $O(n^2)$ ranging operations for a group of n individuals. Furthermore, these systems must schedule collision free ranging operations in a dynamically changing network, which is a significant challenge in power constrained environments such as wearable sensor systems. Pairwise ToF ranging is also possible using acoustic/ultrasonic channels, but these systems suffer from the same scaling and scheduling problems as RF ToF systems.

With the exception of pairwise RF ToF ranging, pure RF sensor systems are unable provide the sub-meter accuracy desired for face-to-face interaction studies. RF ToF meets this target in static indoor environments, but it is unclear what ranging accuracy they achieve in more dynamic indoor environments involving humans. The hardware and power requirements of current RF ToF systems also raise questions about the battery life and form factor of such systems.

In contrast, Opo provides 5 cm ranging accuracy 95% of the time, even at high (60°) angular offsets between interacting people. Opo also offers better battery life than pure RF systems, often by an order of magnitude or more (Table 1), while maintaining a similar form factor to wearable sensors that have been successfully deployed in the 1000s [21, 50].

2.2 TDoA Techniques and Systems

Time-difference-of-arrival systems require both speed of light (RF) and speed of sound (ultrasonic) hardware frontends, but provide an order of magnitude improvement in

ranging accuracy over pure RF systems. However, they are susceptible to obstacle interference, since ultrasonic signals do not propagate through most physical objects.

Smartphone TDoA ranging is accurate to within 5 cm [41]. These systems require phones to be held in certain orientations due to audio directionality and physical object interference. Thus, smartphone TDoA is more suited for applications such as indoor GPS rather than interaction sensing, when phones are often in pockets or purses.

Wearable sensors implement TDoA ranging using radios and ultrasonic hardware to avoid user annoyance. Past system designers have been unable to incorporate the additional hardware and power requirements into infrastructure-free systems. Instead, they have used infrastructure nodes to reduce the resource burden on wearable sensors. Infrastructure nodes can relax the $O(n^2)$ message complexity of pairwise ranging to $O(n)$ by serving as static beacons to mobile receivers, with the resulting range data being used to estimate receiver positions. Such systems include DOLPHIN [36], BAT [23], Guogou [31], and Cricket [46], which rely on a network of infra-red, RF, acoustic, or ultrasonic beacons and receivers, and RADAR [11], which builds and uses a map of RF signal strengths across a building. Custom fabricated broadband ultrasonic systems have been able to provide sub-centimeter localization under heavily controlled environments, with bulky and unwearable nodes [45]. Among infrastructure systems that can be deployed today, it is reasonable to expect up to 10 cm spatial accuracy [23, 46]. Some systems, such as DOLPHIN, report accuracy as high as 2 cm, but only under ideal, static conditions [36].

A better approach to addressing the $O(n^2)$ message complexity of pairwise ranging, without the overhead and co-location errors of infrastructure-based approaches, is to use broadcast (one-to-all) ranging with TDoA between RF and ultrasonic pulses. AHLoS [53], and its successor iBadge [40], offer a decentralized, ad-hoc broadcast ranging scheme. But, AHLoS relies on the underlying synchronization provided by a DSDV [42] variant that is ill-suited to dynamic mobile networks. Hence, it is reduced to a static-

plus-mobile system with infrastructure-dependent synchronization of ranging events. Cricket [46] also employs broadcast ranging. However, it too could not achieve efficient mobile neighbor discovery, and thus uses active, transmitting infrastructure nodes, and passive, listening wearable sensors.

Part of the problem with these systems is exactly how much infrastructure is required. Even deployments which require just a single visible infrastructure node have proven problematic [24]. Localization systems need at least three visible beacons to localize. This is especially problematic for ultrasonic beacons, since they require line of sight to minimize error. The Active Bat system, a RF/UL TDoA localization system, found that 100 infrastructure nodes are required to achieve sufficient coverage in a 280 m^3 office space. Assuming a 3 m ceiling height, this means that they require over 1 node per square meter of ceiling [23].

For a general-purpose interaction sensing system, infrastructure imposes a significant usability barrier. Installing and maintaining infrastructure is laborious and expensive, and limits researchers to characterizing interactions in specific settings. Even if a deployment covers an entire workspace, it is intractable to cover every restaurant, bar, or theater users may visit. As evidence, we cite that infrastructure based deployments have been short, rare, and limited to a room [24], or floor [2], while infrastructure-free smart phones have been deployed to study groups in depth over months at a time [8, 33], and infrastructure-free wearable sensors have been deployed in the thousands across different high schools [21, 50].

Opo provides 5 cm ranging accuracy 95% of the time, even at highly angular (60°) interactions, which is slightly better than current TDoA systems. Opo also improves upon the battery life and form factor of these systems, but where Opo excels in comparison is in its infrastructure-free operation, which drastically increases its usability.

2.3 Discovery, Synchronization, and Wakeup

Our review of localization and interaction sensing systems shows that currently, systems can either be infrastructure-free and spend their power budget on neighbor discovery, or utilize infrastructure and have the power budget to sense interaction distance. Since the creation of many of these systems, various techniques have been proposed to discover and synchronize mobile nodes with duty-cycled radios, including periodic extended transmission [43], listening [16], random [35], and deterministic [26] neighbor discovery. These protocols expose a fundamental power vs latency tradeoff that requires interaction sensing deployments to select between battery life/form factor and temporal fidelity. Based on preliminary, controlled tests, UConnect claims to offer a 2.5 s discovery latency with a 1.3 mW power draw, which is enabled by using 250 μs discovery slots, instead of the 1-2 ms slots common among other protocols [26]. In contrast, our 7-day pilot deployment showed a 1.41 mW power draw while providing TDoA ranging estimates with fewer RF messages. The similar power draw, embedded ranging, and lesser RF congestion make Opo's broadcast synchronization + ranging a superior option to modern neighbor discovery protocols + currently available ranging technology.

Wakeup radios sidestep the power/latency tradeoff inherent in discovery and synchronization protocols. A survey of wakeup radios reveals 20 designs that draw 50+ μW , with receive sensitivity roughly between -100 and -20 dBm, and one design that draws 98 nW with a sensitivity of -41 dBm [49]. However, wakeup radios are still a nascent technology requiring custom fabricated chips, and it is unclear when they will be ready for mass use. Hypothetical interaction sensing systems equipped with wake up radios would still need ultrasonic hardware, so this technology would complement Opo's low power ultrasonic frontends.

Newer UL wakeup circuits [29, 63] offer low power operation. Opo builds on this work by multiplexing a single transducer for UL RX and TX, demonstrating viability with commercial components, improving noise sensitivity, and using ultrasonic wakeups to trigger scalable TDoA ranging.

3 Design Requirements and Targets

Our survey of epidemiology, sociology, psychology, and robotics sets a minimum ranging accuracy of 1 m, with the understanding that there is greater insight to be gained with greater accuracy. Based on current state-of-the-art systems, researchers are interested in a maximum interaction distance of 2 m [21, 50]. Current wearable sensors offer 20 s temporal fidelity, but greater temporal fidelity may be significant in human interactions [54]. We thus set a minimum bar of 20 s temporal fidelity, with the desire to maximize temporal and ranging fidelity without breaking the usability and scalability requirements discussed below.

3.1 Defining Usability

Usability, or the ease and comfort at which a system can be deployed by researchers and used by participants, has proven to be important to an interaction sensing system's real-world prevalence. To set usability requirements, we draw upon past wearable sensor deployments.

Researchers from the University of Utah successfully deployed wearable pure RF proximity sensors called WRENS to over 8,000 school-age children [21]. The authors reported no issues of discomfort or other burdens from participants. We treat the volume and weight of the WREN (13 cm^2 , 10.8 g) as an upper bound for our form factor. The WREN deployment [21] and past TelosB deployments [50] indicate that at minimum, a day-long battery life is needed, although greater battery life is highly desirable. The WREN deployment specifically desired a week-long battery life [21].

The other key property we derive from WREN is the criticality of infrastructure-free operation. Without characterizing the physical space, it is impossible to know exactly how much infrastructure is necessary or where to best place it. Beyond the resource cost of set-up and tear-down, infrastructure-dependency also defines physical boundaries on interaction sensing, making systems less general. Anecdotally, we found in discussions with public health professors that even obtaining permission to set up infrastructure can be a formidable barrier.

For the design of a flexible and practical interaction sensing system, we consider infrastructure an untenable requirement to impose on Opo.

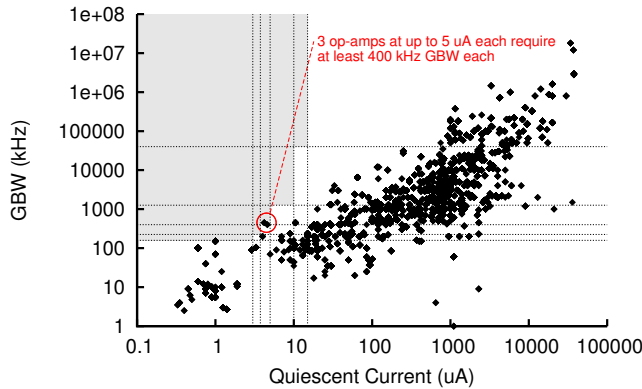


Figure 1: A survey of op-amps comparing power draw and gain. Cascading op-amps results in exponential growth in gain with only a linear growth in power. The shaded gray region contains the gain to power tradeoff from one to five op amps (left-top to right-bottom) normalized against the circled op amp we chose.

3.2 Scalability vs The Common Case

Since a circle 2 m in diameter can only fit 16 average U.S. adults around its perimeter [56], it is not necessary for 1,000 Opos to simultaneously communicate with one another. We optimize Opo for the common case: 2–10 individuals within 2 m of each other, and speculate on ways to scale Opo for hyper-dense scenarios in Section 7.

3.3 Interactions vs Proximity

Current interaction sensing systems often equate proximity with interactions. If a phone’s Bluetooth scan spots another phone, we assume that two people are interacting, even if they are just working in neighboring offices. Intuitively, this assumption is prone to false positives. Furthermore, case studies in disease spread have shown the need for more directional interaction sensing in addition to better interaction distance sensing [19, 60].

The SocioMetric badge mitigates this problem by coupling Bluetooth scans with infrared transceivers to establish that a clear line of sight exists between two people [39]. However, this adds bulk to its form factor, increases power draw, and does not increase ranging accuracy.

Opo and other UL/RF TDoA systems mitigate this problem by exploiting the inherent directionality of UL transducers and the inability of ultrasonic signals to propagate through physical objects such as walls.

4 Opo Design

Opo is designed to provide infrastructure-free interaction distance sensing with better temporal fidelity than past infrastructure-free systems. This is made possible by a novel ultrasonic wakeup radio, which enables an Opo sensor to use broadcast ranging to asynchronously wake up and range with all n neighbors in one interaction. We first introduce our broadcast ranging primitive and then build up our Opo design, starting from the ultrasonic wakeup frontend building block into a complete system.

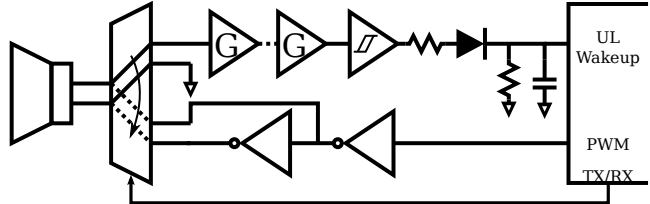


Figure 2: The Opo ultrasonic subsystem is composed of a low-power receive frontend (top) and a simple inverter-driven transmit frontend (bottom). An analog switch controls whether the transducer is transmitting or receiving.

4.1 Asynchronous, Broadcast Ranging

Coordinating wakeups and communication in a highly mobile network is extremely challenging. Traditional neighbor discovery protocols are not designed to be run every second and a centralized architecture violates our infrastructure requirement. Opo solves this problem by avoiding coordination and bi-directional communication.

Opo sensors have an always-on low-power ultrasonic wakeup frontend. An Opo ranging operation begins when one sensor elects to announce its presence by transmitting an ultrasonic pulse. Any sensor that receives this wakeup pulse prepares to receive a range event from the transmitter. A range event is a unidirectional transmission from the transmitter to all n neighbors that receive the signals. At the end of a range event, all receivers know their range from the transmitter. By permitting this asymmetry and avoiding bidirectional communication, Opo enables $1:n$ ranges to be captured per range event, enabling a network of n sensors to calculate all of their mutual ranges in only n range events as opposed to the n^2 events required in pairwise ranging schemes.

4.2 Exponential Gain = Low-Power Wakeup

The key to our broadcast ranging primitive is the always-on ultrasonic wakeup circuit. A piezoelectric ultrasonic transducer will generate a small amount of current when struck by an ultrasonic pulse (the Opo wakeup). The question is whether this tiny current can be reliably and accurately detected within a constrained power budget.

Empirically, we find that a $1000\times$ gain¹ is required to reliably detect the ultrasonic signal. To do this, we scraped the product summaries Digikey provides for its catalog of op-amps. We surveyed 15,000 op-amps that can be run from a typical 3.3V power supply to determine how much power would be required to provide a $1000\times$ gain. Figure 1 explores the tradeoff space between the number of gain stages, the gain of each stage, and the total current draw.

In theory, we can use any number of op-amps in our ultrasonic front end. In practice, we are highly motivated to limit the number of op-amps used. Since filters are imperfect, the noise floor increases exponentially with the number of op-amps, reducing the voltage area (V_{CC} - noise floor) that our system has to work with. In early experiments, even using 4 op-amps required significant fine tuning and additional filtering in the system. Furthermore, adding additional op amps increases our form factor, limiting the wearability

¹This is same gain required in SpiderBat [37].

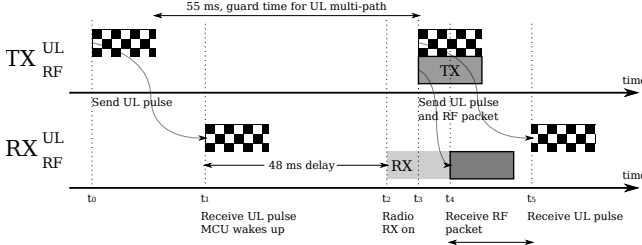


Figure 3: An Opo ranging operation begins with a wakeup UL pulse. Upon receipt, a receiver disables its UL RX frontend and starts a timer and waits for 48 ms for any UL multipath signals to dissipate. The receiver then enables its radio in anticipation of the TDoA signals and starts a 8 ms range-failure timeout. 55 ms after the wakeup pulse, the transmitter sends a simultaneous RF packet and ranging UL pulse. Upon receipt of the RF packet, the receiver re-enables its UL RX frontend and receives the ranging UL pulse. The receiver computes the TDoA between the RF and ultrasonic pulses to calculate its range from the transmitter. If the receiver’s 8 ms range-failure timer triggers before receiving the complete range sequence, it abandons the range operation and returns to idle.

of our sensors. Based on these factors, we limit our search space to 5 op amps. Our survey found that we can achieve a $1000\times$ gain with a 3 stage amplification front end that draws 19 μA when idle. Even using a small, 40 mAh battery, the idle listening current of our UL wakeup front end consumes less than .1% of our power budget over a week long lifetime.

4.3 Ultrasonic Frontend

Figure 2 shows the Opo ultrasonic subsystem. The amplified ultrasonic signal is fed into a comparator and integrator which is connected to a MCU interrupt pin. The MCU also controls an analog switch that can connect the ultrasonic transducer to a transmit frontend for pulse generation.

4.4 Ranging: RF and Ultrasonic TDoA

As our survey of systems in Section 2 shows, pure RF techniques are currently unable to achieve sub-meter resolution. Since Opo already uses an ultrasonic wakeup radio, we build our ranging primitive using the well-studied “thunder and lightning” approach. During a range event, the transmitting sensor sends both an RF packet (speed of light) and an ultrasonic pulse (speed of sound). By comparing the arrival times of these two events, receivers can calculate the time-difference-of-arrival (TDoA) and in turn their range from the transmitter. The transmitter includes a unique ID in the RF packet to identify who is transmitting the range event. Figure 3 shows a complete Opo ranging operation: a wakeup UL pulse followed by the TDoA ranging pair.

4.5 The Unimportance of Congestion Control

An obvious question is how an Opo sensor decides when to transmit and how it avoids TX collisions. In our protocol, each sensor simply waits for a random interval uniformly drawn from 1-3 s with ms granularity between each ranging operation. To provide some intuition for why this simple transmit scheme is sufficient, we examine the possible



(a) Various Opo implementations. The leftmost board is a standalone Opo frontend, designed to act as a daughterboard for standard mote platforms. The center board is the evaluated Opo system. The round board is the next generation Opo, optimized for form factor.



(b) Various different wearing scenarios of Opo. The Opo in the upper left is a shirt button; the Opo in the upper right is a lapel pin; the Opo in the bottom left attaches to a tie clip; the Opo in bottom right is a badge clip.

collisions. Since an Opo range operation takes only around 50 ms, we simplify our analysis by ignoring the effects of sensor mobility during a single ranging operation.

Directionality differentiates the broadcast domain of ultrasonic and RF signals. If two sensors are proximal but not facing each other and choose similar transmit times, a receiver may detect the wrong transmitter’s RF packet, artificially increasing the TDoA from the wrong transmitter. For this collision to occur, the extra packet must arrive after the receiver’s multipath delay and before the actual transmitter’s RF packet—an 8 ms window at most. Collisions can also occur if a new transmitter elects to send its wakeup pulse between the RF and ultrasonic pulses of an ongoing ranging operation. This type of collision would cause a receiver to record an artificially short range with the correct transmitter.

A final type of collision may occur if two sensors elect to transmit at the same time. The impact of such a collision would be a missing ranging event for each sensor, as Opo sensors cannot transmit and receive at the same time.

We hypothesize that for reasonably sized groups, the probability of these collisions is sufficiently low and Opo’s temporal fidelity is sufficiently high to compensate for the few errors that will occur.

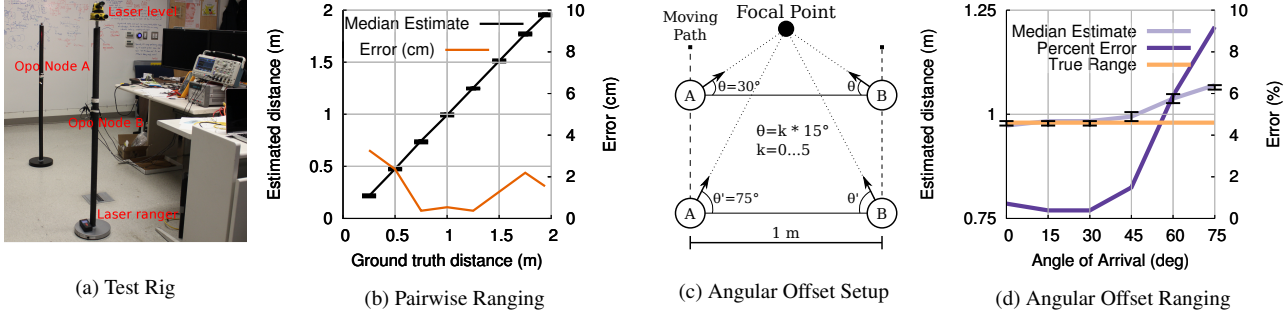


Figure 5: Controlled Microbenchmarks: Our test set up (5a) is comprised of Opo sensors mounted on two metal poles, a laser range finder, and a laser angle finder. 5b shows that our average error is usually < 2 cm. The black bars are the 95% error bars for Opo’s range estimations, showing that Opo is both accurate and precise. To test angular offset performance (people chatting in a circle), we pointed two Opo sensors at the same focal point and slowly increased the angle between them, as shown in 5c. Our results (5d) show that while error does increase with angular offset, average error is only 6% at 60°(six people in a circle).

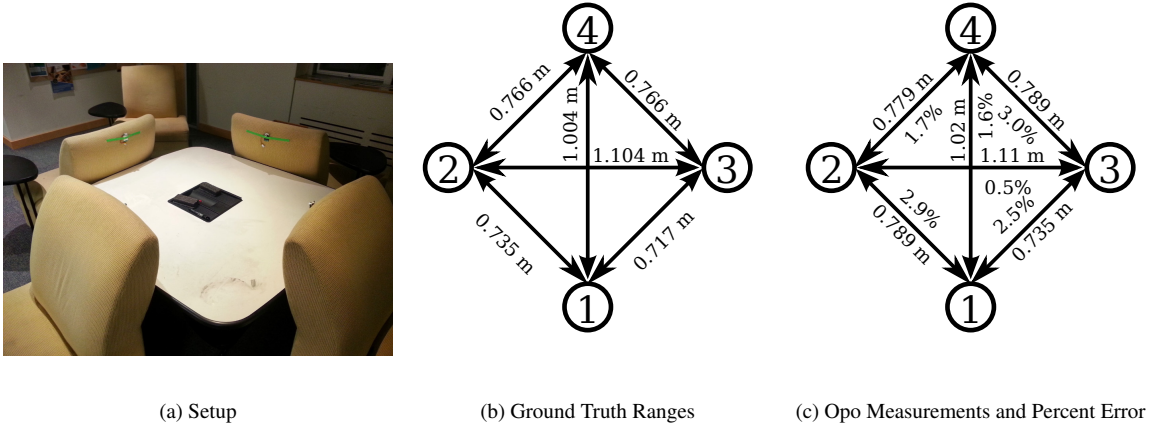


Figure 6: Four-Way Ranging Accuracy: Setup (6a), ground truth (6b), and Opo measurements (6c). The measurements shown in 6c are the median measurements between each pair of sensors, aggregated over the duration of the experiment (12 min).

5 Implementation

To evaluate our design, we implement several generations of the Opo platform, refining the power, performance, and form factor([Figure 4a](#)). In [Figure 4b](#), we show our next-generation Opo in various wearable arrangements.

We built our Opo prototype around the EPIC platform [[17](#)]. From the three candidate op-amps in our survey ([Figure 1](#)), Micrel’s MIC861/863 provides the best amplification to power tradeoff. We select the Prowave 400PT120 transducer for its tight 40 kHz center frequency. We empirically derive the transducer response time to establish a baseline offset and subtract 15 cm from raw TDoA range calculations. Our evaluation in [Section 6.1.1](#) finds our constant offset to be consistent between transducers. Our schematic and software stack are available at github.com/lab11/opo.

We implement the Opo software application as a TinyOS library, enabling easy adaptation by other platforms. Our TDoA calculations assume the speed of light is instantaneous and the speed of sound to be 348.485 m/s.

6 Evaluation

We evaluate Opo’s ranging accuracy, temporal fidelity, and power usage, along with the effects of density on Opo’s performance with a series of controlled tests. We then evaluate Opo’s ability to characterize human interactions with a series of human experiments, testing Opo’s ability to capture both short and long interactions and individual and group interactions. We further show that Opo works for both sitting and standing interactions, and casual and work interactions. Following that, we inspect the energy usage of Opo and develop a power model to inform deployments. We finish our evaluation with a week long deployment with 8 participants to evaluate real-world performance and battery life.

Recalling that an Opo sensor records no information when it transmits, we evaluate Opo with a global perspective. We aggregate all of the collected ranges and consider pairwise metrics using this aggregate view, independent of which sensor was the transmitter or receiver.

6.1 Ranging Microbenchmarks

We use a test rig ([Figure 5a](#)) to conduct a controlled evaluation of ranging accuracy and the effects of angular offsets.

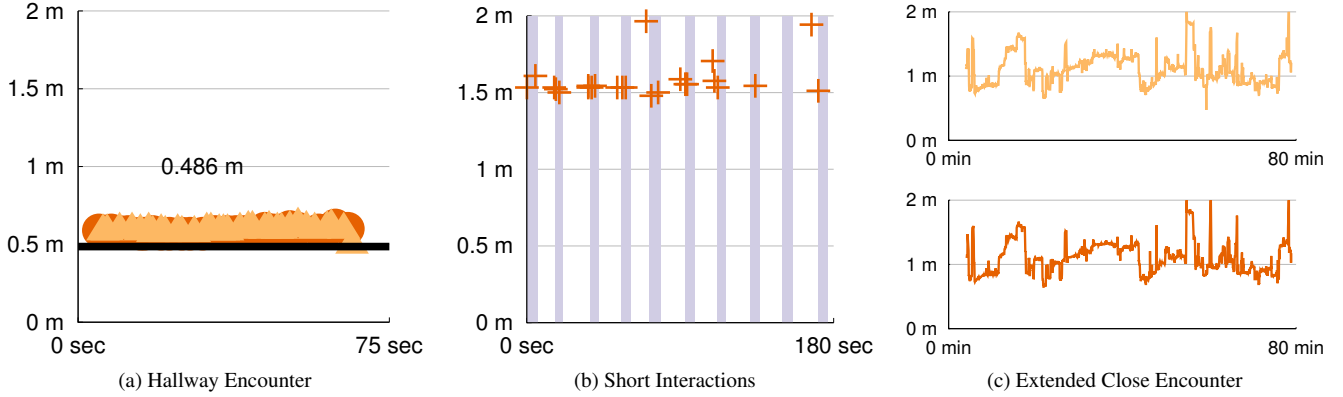


Figure 7: Various Pairwise Human Interactions: 7a shows a typical hallway encounter where two participants walk towards each other in a hallway, stop and chat for 65 s, and then continue on their way. To test Opo’s ability to capture short interactions (7b), two participants stood on either side of a hallway corner. At regular intervals, one participant would turn the corner, face the other for 5 s, then go back to his original side of the corner. As 7b shows, Opo successfully captures the majority of short interactions. 7c shows an extended, professional interaction where two participants sat and collaborated on a project for 75 min. The variations in distance are the result of natural movements, and show what proximity sensing systems miss.

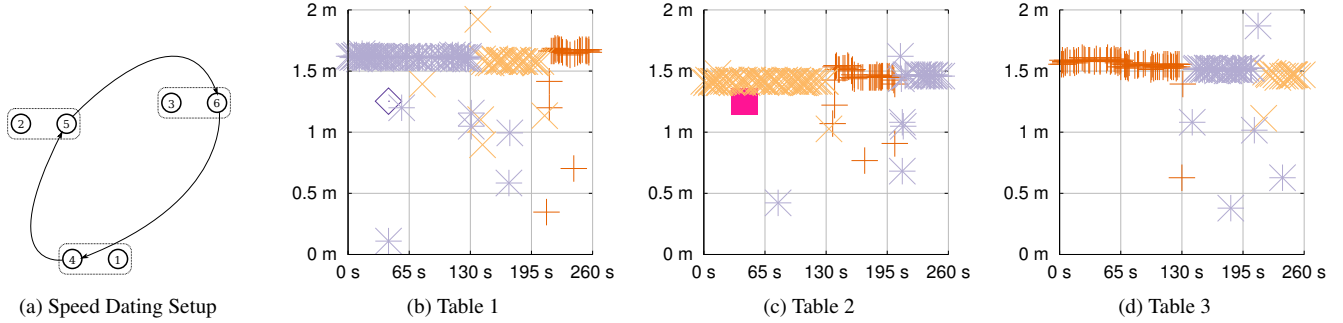


Figure 8: Speed Dating: 3 tables are laid out, with 1 stationary participant sitting at each table, and 3 participants who rotate between tables (8a). Rotation times decrease from roughly 120 to 60 to 45 s. 8b, 8c, 8d represent the interactions at each table, with each rotating participant being represented by a different color and marker. Ground truth is roughly set to 1.5 m, but due to chair position and posture differences, exact error is difficult to determine. However, ranging is precise within interactions, and only 7 of 396 range measurements are unrealistic. Distance variations between interactions are the result of people getting in and out of table chairs.

6.1.1 Pairwise Ranging Accuracy

To evaluate face-to-face accuracy, we perform Opo ranging measurements at a series of distances between 0.25 and 2 m, as shown in Figure 5b (with 95% error bars). We conduct 45 range measurements at each distance and find an average error of 0.015 m. For a given distance, 95% of ranging measurements are within 0.02 m of each other.

To evaluate precision across UL transducers, we take 10 transducers and conduct this test at 2 m, taking 45 measurements with each transducer. We find that 95% of all 450 measurements fall within 0.01 m of each other, with a median range measurement of 2.00 m.

6.1.2 Ranging Errors due to Angular Offsets

In group interactions, people often face the center of the group, leading to symmetrical angular offsets between people. We evaluate the effects of angular offsets on ranging accuracy by sweeping symmetrical offsets from 0° to 75° while keeping distance constant (Figure 5c). We conduct 10 ranging measurements at each angle, and find in Figure 5d

that increasing offsets leads to an increase in measured range. Precision is unaffected, with 95% of ranging measurements at a given angle falling within 0.017 m of each other. Even at a 75° offset, Opo is accurate to within 0.01 m, a generational improvement over the 2 m resolution of RF scans.

6.2 Four-Way Ranging Accuracy

We evaluate Opo’s expected group interaction performance with a four-way interaction test (Figure 6). We find that sensors do not interfere with each other, with median range measurements falling within 3% of the true distance. Sensors report an average 1.5 s temporal fidelity and 82% packet reception rate. Performance is consistent among the four sensors, with packet reception rates between 77% and 86% and average temporal fidelities between 1.48 and 1.59 s.

6.3 Effects of Density

One concern is that sensor density can cause false range measurements through colliding Opo transmissions. We expect these errors to manifest as ranging “spikes”, which

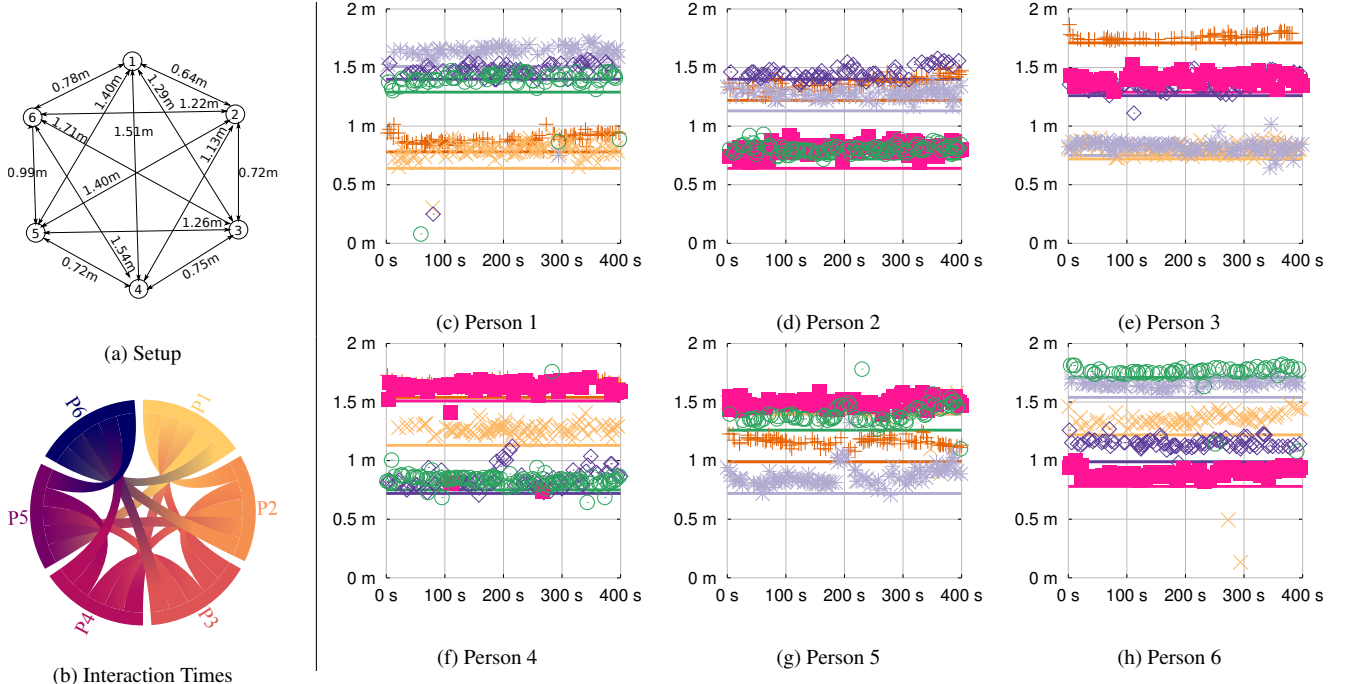


Figure 9: Group Chat: 6 participants stand in a circle and chat for around 6.5 min. The setup and rough ground truth is shown in 9a, although participants naturally moved and shifted during the course of the experiment. In 9b, chords represent interactions between participants, with chord width being based on measured interaction time. 9c-9h show the range measurements from each participant/sensor. Rough ground truth is shown as solid lines. 14 of the 2683 measurements are found to be unrealistic.

would increase the spread of measured distances and decrease ranging accuracy. To evaluate the effects of density on ranging accuracy, we placed 18 sensors facing inwards flush along the sides of a $0.38 \text{ m} \times 0.30 \text{ m} \times 0.27 \text{ m}$ enclosed box for around 12 hr. Ranging accuracy appears to be in line with our microbenchmarks, although we only measured a sampling of the possible sensor pairings. Opo detected 143 of the possible 153 pairings. In all but nine pairings, 90% of the data readings are within .10 m of each other. In 87% of the pairings, 90% of the range measurements are within .05 m of each other. While it is possible that density introduces consistent, systemic error that our sample hand measurements missed, we find this to be highly unlikely. This test shows that even in dense situations, Opo will likely maintain high ranging accuracy. However, density did affect temporal fidelity. Opos in this scenario report a 8.4 s temporal fidelity. This is expected, since in the current Opo implementation, sensors do not take into account the time they spend receiving, writing to flash, etc, when setting their transmit timers. However, this is still a 2x improvement over the 20 s temporal fidelity of currently deployed interaction sensing systems.

6.4 Capturing Human Interactions

To evaluate human interaction sensing, we perform a series of short experiments with six participants. Participants are given as much freedom as possible without breaking the overall flow of the experiments, meaning we only have a rough sense of ground truth distances.

We evaluate temporal fidelity by examining the time between ranging measurements and ranging accuracy through

cross-validation of ranging trends. If only one sensor reports a significant change in range, it is likely a false measurement.

6.4.1 Figure 7a: Hallway Conversation

Our first test is a simple hallway conversation to establish that the ranging accuracy from our microbenchmarks carries over to real face-to-face interactions. Two participants walk towards each other, converse for 65 s, and then part ways. Opo sensors report an interaction time of 60 s, a packet reception rate of 98%, and an average of 1.07 s between packets. This matches our ideal temporal fidelity of 1.0 s for a transmit period of 2 s. We find an average range measurement of 0.525 m with a standard deviation of .018 m. True range is roughly 0.49 m, leaving us with a 0.035 m error.

6.4.2 Figure 7b: Short Interactions

To evaluate Opo’s ability to capture short, spurious interactions, we perform ten 5 s interactions. To do so, we have two participants stand on each side of a hallway corner, with one periodically turning the corner to interact for 5 s, then returning to his side of the corner. We successfully capture 9 out of the 10 interactions. Our total sensed interaction time is 36 s, which is in line with expectations. While not perfect, Opo’s ability to capture short spurious interactions represents a significant upgrade from the current 20 s temporal fidelity of RF scanning sensors.

6.4.3 Figure 7c: Close Encounters

To demonstrate the detail that is lost with lower temporal fidelity and proximity sensing instead of range measurements, two participants collaborate on a project for 75 min. Deviations are observed at each sensor, which we attribute to

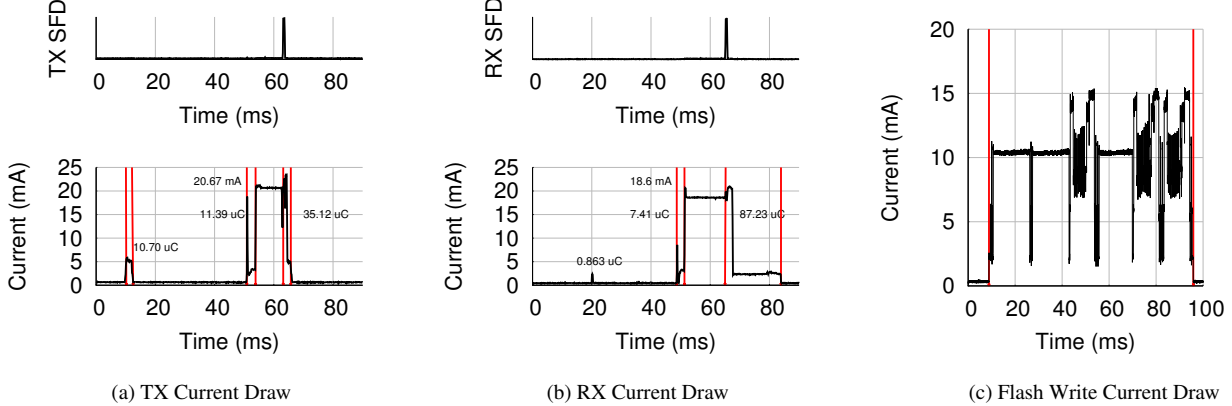


Figure 10: Current Draw Traces: Red lines represent various components (UL TX frontend, radio, mcu, flash) waking up and performing tasks. In 10a, the high current draw time between 53-62 s is due to a radio driver inefficiency. The ranging reception shown in 10b is done at 6 m to increase the visibility of the high powered, radio reception state. The SFD graphs for 10a and 10b show when the relevant radio transmission and reception actually occur. The smaller current spikes occurring before 50 s in 10a and 10b are from the UL frontends and MCU waking up, while the larger current spikes are from the radio turning on.

natural movements – leaning in to discuss details, reclining in chairs, and other common actions. This test exemplifies the type of spatial and temporal detail that Opo is capable of providing over state-of-the-art infrastructure-free systems.

6.4.4 *Figure 8: Speed Dating*

In spaces such as study rooms and coffee shops, there may be multiple pairwise face-to-face interactions within the same general area. To evaluate Opo’s ability to characterize individual interactions within the same general space, we perform a speed dating experiment. We set up three speed dating tables, with three stationary participants and three participants rotating between tables. The duration shortens with each rotation, going from roughly 120 to 60 to 45 s.

We observe an average temporal fidelity of 1.66 s and packet reception rate of 90%, which is in line with our hallway and short interaction tests. Seven out of the nine “dates” are sensed to within 5 s of their true duration. However, two of the 120 second dates are sensed as 108 and 100 seconds. In one of these dates, we found that one participant held his hands in front of his sensor for part of the interaction, causing a gap in range measurements. We speculate that the other interaction error is from a similar cause.

It is difficult to definitively pinpoint false ranges. As people get in and out of seats, we see spikes in interaction distance, which is expected. Other spikes may be caused by people leaning forward or rolling their seats. However, 7 of the 396 range measurements are unrealistic.

6.4.5 *Figure 9: Group Chat*

We evaluate Opo’s ability to capture real group interactions with a 6.5 min six person group chat. Figure 9b shows that Opo accurately senses that six people are all interacting with each other for the same amount of time. Each colored arc represents a different participant, with chords representing interactions between connecting participants. Chord width is determined by the total sensed interaction time between two connecting participants.

Spatially, there is a 0.07 m standard deviation in pairwise

range measurements. Based on empirical observations, spatial deviations over 0.5 m are likely incorrect range measurements. From a total of 2683 range measurements, we find 14 false ranges. Temporally, we see an average 2.3 s temporal fidelity among pairs of sensors and an average packet reception rate of 80%. Lower packet reception rates are unsurprising since we observe that in group situations people will sometimes turn towards a specific person. As discussed in Section 6.3, temporal fidelity falls with density.

6.5 Energy Costs and Model

To evaluate expected battery life, we first calculate the energy cost of each Opo operation. We use these costs to inform a basic energy model from which we extrapolate lifetime estimates. We have not previously discussed data offloading as it is not central to the design of Opo. However, we would be negligent to omit data offloading from our energy model. In this analysis, we assume batch offloading and only burden Opo sensors with storing measurements to flash.

6.5.1 Energy Costs

Figure 10 captures power traces of each of Opo’s fundamental operations. We examine these in detail here.

Opo Ranging Transmission:

$$\begin{array}{rcl} E_{UL_PULSE} & = & 35.31 \mu J \\ + E_{TDOA_PULSES} & = & 784.7 \mu J \\ \hline E_{TX} & = & 820 \mu J \end{array}$$

Due to software inefficiencies, the energy required to send an RF packet is artificially high. The default TinyOS CC2420 driver uses a 9 ms backoff timer—time 53 to 62 in Figure 10a—when transmitting a packet, where the radio is in a high power receive state. While this is helpful in synchronized sensor networks, this backoff timer serves no purpose for Opo. We estimate that modifying the driver and getting rid of the backoff timer would save 564 μ J of energy², a 72% reduction. However, due to time and labor constraints, we were unable to get a modified CC2420 driver working.

² $(18.8 \text{ mA} - 426 \mu\text{A}) \times 3.3 \text{ V} \times 9.3 \text{ ms} = 564 \mu\text{J}$

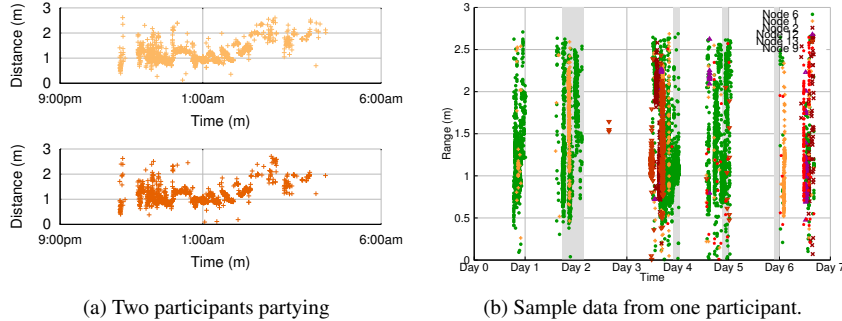


Figure 11: Real-World Deployment: 11a shows Opo measurements from two participants during a party. Measurements from one participant’s sensor is consistently validated by measurements from the other participant’s sensor. 11b shows sample data from one participant. The shaded areas are time spent by the participant in uninstrumentable spaces (e.g. restaurants).

Opo Ranging Reception:

$$\begin{aligned}
 E_{MCU_UL_INTERRUPT} &= 2.85 \mu J \\
 + E_{RF_IDLE_LISTEN} &= 61.4 mW \times (range) ms \\
 + E_{RF_PACKET} &= 184.4 \mu J \\
 + E_{PROCESSING} &= 127.9 \mu J \\
 \hline
 E_{RX_RANGE} &= 315.2 \mu J + E_{RF_IDLE_LISTEN}
 \end{aligned}$$

The energy consumed idly listening by the RF frontend will vary as a function of the distance between the transmitter and receiver. Figure 10b shows a 6 m range to exaggerate this effect and clearly identify the RX idle listening time.

Write Batch of Range Data to Flash:

$$E_{WRITE_FLASH} = 2.83 \text{ mJ}$$

Our Opo implementation writes flash in 36-sample³ batches. Thus, to get the actual cost of a range reception:

$$E_{RX} = E_{RX_RANGE} + \frac{E_{WRITE_FLASH}}{36} = 393.8 \mu J + E_{RF_IDLE_LISTEN}$$

Static Power While Idle:

$$P_{IDLE} = 148.5 \mu W$$

In idle mode, Opo is in its lowest-power state. The radio is powered off, the MCU is in deep, RAM-preserving sleep, and only the ultrasonic wakeup circuit is powered.

6.5.2 Energy Model

To reason about energy, we make a simplifying assumption that there is no packet loss. Our analysis double-counts Opo’s static power draw as baseline power was not removed from individual energy costs. As the idle power is 10 – 20x lower than the active power and Opo’s duty cycle is relatively low, the impact on our model is not significant.

We begin with the simplest case: two sensors facing one another. Every two seconds, each sensor will perform one ranging transmission and one ranging reception. We can express the energy each sensor consumes as a function of time t and average distance d_{avg} between the sensors:

$$\begin{aligned}
 E_n(t, d_{avg}) &= t \times 148.8 \mu W + t \times \frac{1 \text{ range}}{2 \text{ sec}} \times \\
 &(820 \mu J + 393.8 \mu J + 315.2 \mu J + 61.4 mW \times d_{avg})
 \end{aligned}$$

³ $\frac{512 \text{ bytes}}{\text{page}} / \frac{14 \text{ bytes}}{\text{record}} = 36 \text{ records per page.}$

Next, we extend our model to include multiple sensors. Our aim is to place an upper bound on energy consumption. Opo consumes the most energy when it sees the greatest number of sensors (more ranging receptions). Our model takes this to its natural extreme, $n + 1$ sensors arranged such that all $n + 1$ sensors are facing one another (e.g. in a circle):

$$\begin{aligned}
 E_n(t, d_{avg}, n) &= t \times 148.8 \mu W + t \times \frac{1 \text{ range}}{2 \text{ sec}} \times \\
 &(820 \mu J + n \times (393.8 \mu J + 315.2 \mu J + 61.4 mW \times d_{avg}))
 \end{aligned}$$

6.5.3 Lifetime Estimation

We consider a hypothetical deployment with an average of 5 visible sensors, 2 meters (6 ms RX) average range, and 8 hours of interaction per day. In this setting, each Opo sensor would consume about 126 J of energy per day. A week-long deployment would require a 66 mAh battery.

6.6 Real-World Deployment

To validate Opo’s real-world operation, we deployed Opo sensors among eight participants for a week. This deployment produced 47,189 range measurements. Sensors had an average battery life of 93 hours, or 11.6 business days, on a 40 mAh battery the size of a dime. Sensors used an average of 137 J a day, compared with the 126 J from our model.

Establishing ground truth proved challenging. Not all participants were comfortable with video taped ground truth, and efforts to log all interactions in journals quickly proved untenable, even among just eight people. Generally speaking, we see clustering of ranges and cross validation of ranging estimates similar to that seen in our extended close encounter experiment (Figure 7c). A 9 hour slice of time where two participants partied together is shown in Figure 11a as an example of this clustering and cross validation. We find a median 5 s temporal fidelity, as opposed to the 1 s ideal, which is still a 4x improvement over current interaction sensing systems. Participants wore the sensors using both lanyards and magnetic clips, and reported no discomfort.

Even in this short deployment we see the importance of infrastructure-free operation. Figure 11b shows the results from one participant, who spent 2 days entirely outside of academic settings, which is shown as gray shaded areas.

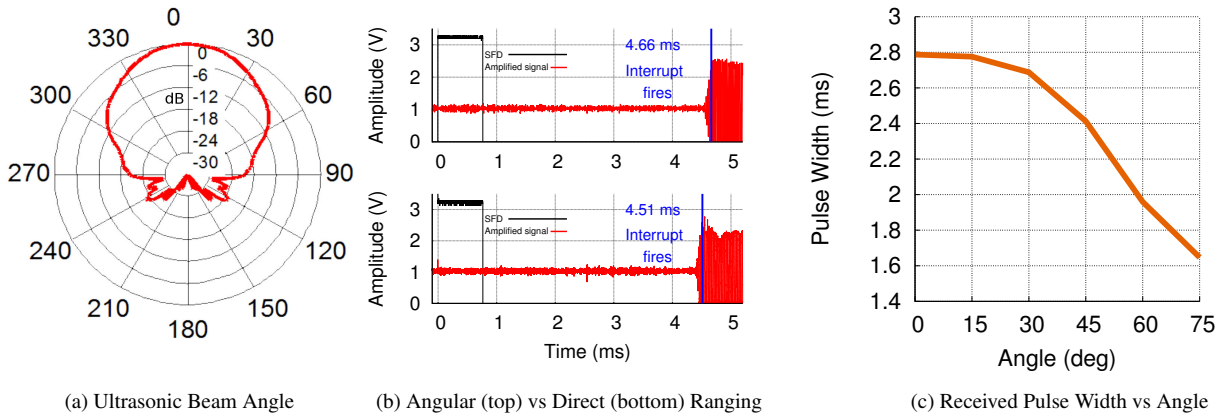


Figure 12: Effects of Angle of Arrival.

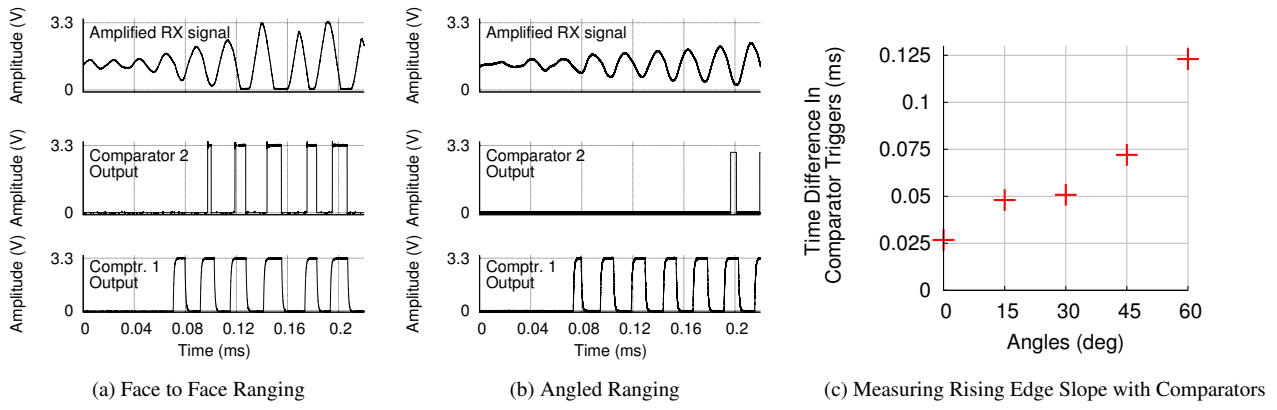


Figure 13: Exploring Ultrasonic Rise Time

Even on days where participants were in possibly instrumentable buildings during the day, significant time was spent in other uninstrumentable areas, such as restaurants during dinner, bars after work, etc.

7 Discussion

We revisit some limitations of our design, present possible alternatives, and discuss future improvements.

7.1 Reducing Angular Offset Errors

In Section 6.1.2, we show that angular offsets between sensors, like those among adjacent people standing in a circle, increase ranging error. This occurs because the ultrasonic transducer’s transmit power and receive sensitivity decrease with offset, as shown in Figure 12a. This results in a delayed received ultrasonic rise time, leading to a delayed timing capture, which is interpreted as a longer range. Figure 12b illustrates this delay by comparing the output of the amplified ultrasonic signal received under face-to-face (bottom) and high angular offset ranging (top). The angular offset causes a 150 μ s delay, which results in a 5 cm estimation error at room temperature. The reduced signal strength also results in a shorter pulse length. Figure 12c shows that pulse length decreases with an increase in angular offset. We hypothesize that the reduced power at angular offsets manifests as a longer time for the transducer to reach resonance.

Measuring pulse duration in heavy multipath settings may be challenging as reflections can extend the received pulse duration. An alternate approach to detecting angular offsets could be to estimate the slope of the envelope of the received ultrasonic signal using two comparators with different voltage thresholds. Figure 13a shows the received signal and the output of two comparators with two different thresholds for a head-on range. Figure 13b shows the same signals for a 60° offset angle range, simulating six people standing in a circle. Our limited testing (Figure 13c) shows an inverse relationship between comparator trigger time differentials and angular offset. This suggests future work could incorporate this technique to reduce offset angle-induced errors.

7.2 Neighbor Density vs Data Fidelity

Currently, Opo attempts to transmit ranging packets at a fixed average rate (with randomized transmission times) regardless of neighborhood density. The rationale behind this approach is that in most social settings, only a small number of people will occupy an area of 2 m around a person, so it is preferable to have high temporal fidelity. However, in dense situations it may be preferable to trade temporal fidelity for scalability. For example, an alternate design could reset Opo’s transmit timer every time a reception occurs, causing temporal fidelity to drastically decrease with density.

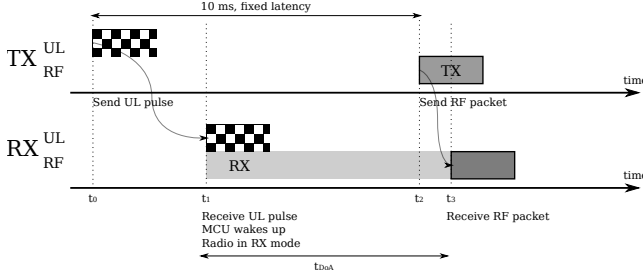


Figure 14: A possible future optimization of Opo’s ranging operation. The second ultrasonic pulse is eliminated, calculating the TDoA instead between the wakeup pulse and the subsequent RF packet. The delay for sending the RF ranging packet is also reduced (40 ms to 10 ms). A 10 ms ultrasonic wakeup window covers approximately 3 m of ranging. Sensors further away would miss the radio packet as they would wake up too late to receive it.

A more efficient protocol could also increase scalability. The protocol shown in Figure 14 cuts the UL multi-path guard time, which dominates transmit/receive duration, in half, doubling the number of transmit slots in each period.

7.3 Power Draw Optimizations

The Opo architecture is low-power, but several of our design/implementation decisions reflect pragmatic concerns rather than optimal power choices. Some areas for improvements include the choice of radio, the ultrasonic amplification gain, and fixed vs adaptive transmission rate.

Opo uses the TI CC2420 radio, which draws 18.8 mA during receive and 17.4 mA during transmit (0 dBm) because reference designs and source code are readily available for it. However, lower power radios exist. For example, the LTC5901/02 draws 4.5 mA during receive and 5.4 mA during transmit (0 dBm). Using this radio could lead to a 4x reduction in receive and a 3x reduction in transmit power. Since radio energy accounts for 75% of sensor energy usage, changing the radio could increase sensor lifetime by weeks. Software optimizations could also result in power reductions. We estimate the transmission energy could be reduced from approximately 850 μ J to 300 μ J by eliminating the backoff timer and implementing various other optimizations [16].

Opo’s ultrasonic receive signal chain amplifies the output of the transducer by a factor of 1,000. This gain allows Opo to detect other sensors at large angular offsets, but it also increases Opo’s effective ultrasonic wake-up range. Thus, far away sensors can wake each other up, leading to increased power draw due to spurious wake-ups from distant sensors. Reducing the ultrasonic gain would reduce the range at which sensors can cause spurious wake-ups, but also reduces Opo’s ability to capture group interactions.

We observe that sensors cause these spurious wake ups symmetrically. For every spurious wake up sensor Y causes for sensor X, sensor X also causes one for sensor Y. It may be possible to implement a backoff scheme based on the frequency of spurious wake ups a sensor experiences. This scheme would allow for sensors to trade off temporal fidelity for power usage without sacrificing angular performance.

7.4 Data Collection

Currently, Opo logs data to local flash memory (64 Mb), and data is manually downloaded after an experiment. We have also implemented wirelessly re-transmitting the received data on a different channel immediately, or whenever a base station is detected, using a custom CC2520 adapter board attached to a Raspberry Pi as a base station. Due to the usability barriers of infrastructure, we are exploring using Bluetooth Low Energy to offload data from Opo sensors to smartphones, which can then upload the data to the cloud.

8 Conclusions

Face-to-face interactions are important in many settings, but unobtrusively and efficiently capturing them for study has remained notoriously difficult. In this paper, we present a low-power system that can sense face-to-face interaction distance in an infrastructure-free manner. Having validated the design’s power and performance, we are planning to deploy the sensors at scale in various school and university settings. The key element that enables this work is a new ultrasonic wakeup frontend that can be built from commodity components. With very low power draw, sensors can be miniaturized to the point that they are the size of a large lapel pin, yet keep a 4-day lifetime with a 40 mAh battery. This enables us to keep power-hungry radios mostly off without resorting to duty-cycled neighbor discovery protocols that sacrifice discovery latency to achieve low power. The power and bandwidth requirements of our combined ultrasonic/radio broadcast ranging scale linearly with the number of co-located sensors, whereas pairwise approaches like two-way time-of-flight ranging scale quadratically. Collectively, this work shows that ultrasonic wakeup is viable using commodity components and that small and low power sensor tags can be built around this new capability. Two decades of research have shown that high-power, mobile systems are not difficult to design and low-power, static ones are possible with careful design, but that low-power, mobile networks presents many challenges. In this paper, we show that low-power, computational jewelry is now viable for capturing face-to-face interaction distance, instead of just proximity. This will finally allow us to capture face-to-face interactions with higher spatial and temporal fidelity than ever before, enabling unprecedented research in a variety of fields.

9 Acknowledgments

This work was supported in part by the TerraSwarm Research Center, one of six centers supported by the STARnet phase of the Focus Center Research Program (FCRP), a Semiconductor Research Corporation program sponsored by MARCO and DARPA. This material is based upon work partially supported by the National Science Foundation under grants CNS-0964120, CNS-1111541, and CNS-1350967, and generous gifts from Intel and Texas Instruments.

10 References

- [1] TelosB Mote Platform. http://www.willow.co.uk/TelosB_Datasheet.pdf.
- [2] Cricket Web Page. <http://cricket.csail.mit.edu/>, 2005.
- [3] Limiting Spread: Limiting the Spread of Pandemic, Zoonotic, and Seasonal Epidemic Influenza, 2010.
- [4] Smartphones in the Hands of the Youngest Demographic. <http://emarketer.com/Article/Smartphones-Hands-of-Youngest-Demographic/1009915>, 2013.

- [5] Mobile Technology Fact Sheet. <http://www.pewinternet.org/fact-sheets/mobile-technology-fact-sheet/>, 2014.
- [6] Smartphone Penetration Tops 65% of the US Mobile Market in Q4 2013. <http://www.marketingcharts.com/online/smartphone-penetration-tops-65-of-the-us-mobile-market-in-q4-2013-39595/>, 2014.
- [7] Teens & Technology: Understanding the Digital Landscape. <http://www.pewinternet.org/files/2014/03/Teens-and-Tech-Basics.GWU022514.FIN.POST.pdf.pdf>, 2014.
- [8] N. Aharony, C. Ip, W. Pan, and A. Pentland. The Friends and Family Mobile Phone Study: Initial Report. In *Proceedings of the Workshop on the Analysis of Mobile Phone Networks (NetMob)*, 2010.
- [9] N. Aharony, W. Pan, C. Ip, I. Khayal, and A. Pentland. Social fMRI: Investigating and Shaping Social Mechanisms in the Real World. *Pervasive and Mobile Computing*, 7(6):643–659, 2011.
- [10] E. M. V. Allison E. Aiello. eX-FLU: A Social Network Intervention For Reducing Respiratory Infectious Illness Transmission. <http://www.screencast.com/t/pBxndEk65m>, 2013.
- [11] P. Bahl and V. N. Padmanabhan. RADAR: An In-building RF-based User Location and Tracking System . In *Proceedings of 19th Annual Joint Conference of the IEEE Computer and Communications Societies*. IEEE, 2000.
- [12] C. Beaulieu. Intercultural Study of Personal Space: A Case Study. *Journal of applied social psychology*, 34(4):794–805, 2004.
- [13] P. Beutels, Z. Shkedy, M. Aerts, and P. Van Damme. Social Mixing Patterns for Transmission Models of Close Contact Infections. *Epidemiology & Infection*, 134(6):1158–1166, Dec. 2006.
- [14] N. Bruno and M. Muzzolini. Proxemics Revisited: Similar Effects of Arms Length on Men’s and Women’s Personal Distances. *Journal of Psychology*, 1(2):46–52, 2013.
- [15] C. Cattuto et al. Dynamics of Person-to-Person Interactions from Distributed RFID Sensor Networks. *PLoS One*, 5(7), July 2010.
- [16] P. Dutta et al. Design and Evaluation of a Versatile and Efficient Receiver-Initiated Link Layer for Low-Power Wireless. In *Proceedings of the 8th ACM Conference on Embedded Networked Sensor Systems (SenSys)*, pages 1–14. ACM, 2010.
- [17] P. Dutta, J. Taneja, J. Jeong, X. Jiang, and D. Culler. A Building Block Approach to Sensorset Systems. In *In Proceedings of the Sixth ACM Conference on Embedded Networked Sensor Systems (SenSys)*, 2008.
- [18] N. Eagle, A. S. Pentland, and D. Lazer. Inferring Friendship Network Structure by Using Mobile Phone Data. *Proceedings of the National Academy of Sciences*, 106(36):15274–15278, 2009.
- [19] S. K. H. et al. A Comprehensive Breath Plume Model for Disease Transmission via Expiratory Aerosols. *PLoS One*, 7(5), May 2012.
- [20] G. W. Evans and R. E. Werner. Crowding and Personal Space Invasion on the Train: Please Don’t Make Me Sit in the Middle. *Journal of Environmental Psychology*, 27(1):90–94, 2007.
- [21] A. Forys, K. Min, T. Schmid, W. Pettey, D. Toth, and M. Leecaster. WRENMining: Large-Scale Data Collection for Human Contact Network Research. In *Proceedings of First International Workshop on Sensing and Big Data Mining*, pages 1–6. ACM, 2013.
- [22] Y. Fukuhara, M. Minami, H. Morikawa, and T. Aoyama. DOLPHIN: An Autonomous Indoor Positioning System in Ubiquitous Computing Environment. In *The Workshop on Software Technologies for Future Embedded and Ubiquitous Systems (SEUS)*, 2003.
- [23] A. Harter, A. Hopper, P. Stiegles, A. Ward, and P. Webster. The Anatomy of a Context-Aware Application. *Wireless Networks*, 8(2):187–197, 2002.
- [24] L. Isella et al. Close Encounters in a Pediatric Ward: Measuring Face-to-Face Proximity and Mixing Patterns with Wearable Sensors.
- [25] Z. Jianwu and Z. Lu. Research on Distance Measurement Based on RSSI of ZigBee. In *Computing, Communication, Control, and Management, 2009. CCCM 2009. ISECS International Colloquium on*, volume 3, pages 210–212. IEEE, 2009.
- [26] A. Kandhalu, K. Lakshmanan, and R. R. Rajkumar. U-Connect: A Low-latency Energy-efficient Asynchronous Neighbor Discovery Protocol. In *Proceedings of the 9th ACM/IEEE International Conference on Information Processing in Sensor Networks (IPSN)*, pages 350–361. ACM/IEEE, 2010.
- [27] M. A. Kazandjieva et al. Experiences in Measuring a Human Contact Network for Epidemiology Research. In *Proceedings of the 6th Workshop on Hot Topics in Embedded Networked Sensors*, page 7. ACM, 2010.
- [28] S. Lanzisera and K. S. Pister. Burst Mode Two-Way Ranging with Cramer-Rao Bound Noise Performance. In *Global Telecommunications Conference*, 2008.
- [29] E. Lattanzi, M. Dromedari, V. Freschi, and A. Bogliolo. A Sub- μ A Ultrasonic Wake-Up Trigger with Addressing Capability for Wireless Sensor Nodes. *ISRN Sensor Networks*, 2013.
- [30] Y. Lee, Y. Ju, C. Min, S. Kang, I. Hwang, and J. Song. Comon: Cooperative Ambience Monitoring Platform with Continuity and Benefit Awareness. In *Proceedings of the 10th international conference on Mobile systems, applications, and services*, pages 43–56. ACM, 2012.
- [31] K. Liu, X. Liu, and X. Li. Guoguo: Enabling Fine-grained Indoor Localization via Smartphone. In *MobiSys ’13: Proceeding of the 11th Annual International Conference on Mobile Systems, Applications, and Services*, pages 235–248, 2013.
- [32] A. C. Lowen, S. Mubareka, T. M. Tumpey, A. García-Sastre, and P. Palese. The Guinea Pig as a Transmission Model for Human Influenza Viruses. *Proceedings of the National Academic of Sciences of the United States of America*, 103(26), June 2006.
- [33] A. Madan et al. Social Sensing for Epidemiological Behavior Change. In *Proceedings of the 12th ACM international conference on Ubiquitous computing*, pages 291–300. ACM, 2010.
- [34] C. McCall et al. Proxemic Behaviors as Predictors of Aggression Towards Black (but not White) Males in an Immersive Virtual Environment. *Social Influence*, 4(2):138–154, 2009.
- [35] M. J. McGlynn and S. A. Borbash. Birthday Protocols for Low Energy Deployment and Flexible Neighbor Discovery in Ad Hoc Wireless Networks. In *Proceedings of the 2nd ACM International Symposium on Mobile Ad hoc Networking & Computing*. ACM, 2001.
- [36] M. Minami, Y. Fukuhara, K. Hirasawa, S. Yokoyama, M. Mizumachi, H. Morikawa, and T. Aoyama. DOLPHIN: A Practical Approach for Implementing a Fully Distributed Indoor Ultrasonic Positioning System. In *UbiComp 2004: Ubiquitous Computing*, pages 347–365. Springer, 2004.
- [37] G. Oberholzer, P. Sommer, and R. Wattenhofer. SpiderBat: Augmenting Wireless Sensor Networks with Distance and Angle Information. In *10th International Conference on Information Processing in Sensor Networks (IPSN)*, pages 211–222. IEEE, 2011.
- [38] M. O’Dell et al. Lost in Space or Positioning in Sensor Networks. In *REALWSN*, volume 5, 2005.
- [39] D. O. Olgún, B. N. Waber, T. Kim, A. Mohan, K. Ara, and A. Pentland. Sensible Organizations: Technology and Methodology for Automatically Measuring Organizational Behavior. *IEEE Transactions on Systems, Man, and Cybernetics, Part B: Cybernetics*.
- [40] S. Park, I. Locher, A. Savvides, M. Srivastava, A. Chen, R. Muntz, and S. Yuen. Design of a Wearable Sensor Badge for Smart Kindergarten. In *Proceedings of the 6th International Symposium on Wearable Computers. (ISWC)*, pages 231–238. IEEE, 2002.
- [41] C. Peng, G. Shen, Y. Zhang, Y. Li, and K. Tan. BeepBeep: A High Accuracy Acoustic Ranging System using COTS Mobile Devices. In *Proceedings of the 5th international conference on Embedded networked sensor systems*, pages 1–14. ACM, 2007.
- [42] C. E. Perkins and P. Bhagwat. Highly Dynamic Destination-Sequenced Distance-Vector Routing (DSDV) for Mobile Computers. In *Proceedings of the conference on Communications architectures, protocols and applications*. ACM, 1994.
- [43] J. Polastre, J. Hill, and D. Culler. Versatile Low Power Media Access for Wireless Sensor Networks. In *Proceedings of the 2nd ACM Conferences on Embedded Networked Sensor Systems*, pages 95–107. ACM, 2004.
- [44] C. Poletto, M. Tizzoni, and V. Colizza. Heterogeneous Length of Stay of Hosts Movements and Spatial Epidemic Spread. *Scientific reports*, 2, 2012.
- [45] J. C. Prieto et al. Performance Evaluation of 3D-LOCUS Advanced Acoustic LPS. *Instrumentation and Measurement, IEEE Transactions on*, 58(8):2385–2395, 2009.
- [46] N. B. Priyantha, A. Chakraborty, and H. Balakrishnan. The Cricket Location-Support System. In *Proceedings of the 6th annual international conference on Mobile computing and networking*

- (*MobiCom*). ACM, 2000.
- [47] R. M. Puhl and J. D. Latner. Stigma, Obesity, and the Health of the Nation's Children. *Psychological bulletin*, 133(4):557, 2007.
 - [48] E. Rea et al. Duration and Distance of Exposure are Important Predictors of Transmission among Community Contacts of Ontario SARS Cases. *Epidemiology and infection*, 135(06):914–921, 2007.
 - [49] N. E. Roberts and D. D. Wentzloff. A 98 nW Wake-up Radio for Wireless Body Area Networks. In *IEEE Radio Frequency Integrated Circuits Symposium (RFIC)*, pages 373–376, June 2012.
 - [50] M. Salathé, M. Kazandjieva, J. W. Lee, P. Levis, M. W. Feldman, and J. H. Jones. A High-Resolution Human Contact Network for Infectious Disease Transmission. *Proceedings of the National Academy of Sciences (PNAS)*, 107(51):22020–22025, 2010.
 - [51] M. Salathé, M. Kazandjieva, J. W. Lee, P. Levis, M. W. Feldman, and J. H. Jones. A High-Resolution Human Contact Network for Infectious Disease Transmission - Supporting Information. *Proceedings of the National Academy of Sciences (PNAS)*, 107(51):22020–22025, 2010.
 - [52] T. Sathyam, D. Humphrey, and M. Hedley. WASP: A System and Algorithms for Accurate Radio Localization Using Low-Cost Hardware. *IEEE Transactions on Systems, Man, and Cybernetics, Part C: Applications and Reviews*, 41(2):211–222, 2011.
 - [53] A. Savvides, C.-C. Han, and M. B. Srivastava. Dynamic Fine-Grained Localization in Ad-hoc Networks of Sensors. In *Proceedings of the 7th annual international conference on Mobile computing and networking (MobiCom)*, pages 166–179. ACM, 2001.
 - [54] J. Stehlé et al. Simulation of an SEIR Infectious Disease Model on the Dynamic Contact Network of Conference Attendees. *BMC medicine*, 9(1):87, 2011.
 - [55] E. Stephan, N. Liberman, and Y. Trope. Politeness and Psychological Distance: a Construal Level Perspective. *Journal of personality and social psychology*, 98(2):268, 2010.
 - [56] H. W. Stoudt. *Skinfolds, Body Girths, Biaxial Diameter, and Selected Anthropometric Indices of Adults, United States, 1960-1962*. 1970.
 - [57] N. M. Sussman and H. M. Rosenfeld. Influence of Culture, Language, and Sex on Conversational Distance. *Journal of Personality and Social Psychology*, 42(1):66, 1982.
 - [58] M. Walters et al. The Influence of Subjects' Personality Traits on Personal Spatial Zones in a Human-Robot Interaction Experiment. In *Robot and Human Interactive Communication, 2005. ROMAN 2005. IEEE International Workshop on*, pages 347–352. IEEE, 2005.
 - [59] M. Walters et al. Avoiding the Uncanny Valley: Robot Appearance, Personality and Consistency of Behavior in an Attention-Seeking Home Scenario for a Robot Companion. *Autonomous Robots*, 24(2):159–178, 2008.
 - [60] W. Wells. On Air-Borne Infection. Study II. Droplets and Droplet Nuclei. *American Journal of Hygiene*, 20:611–618, 1934.
 - [61] T.-W. Wong, C.-K. Lee, W. Tam, J. T.-F. Lau, T.-S. Yu, S.-F. Lui, P. K. Chan, Y. Li, J. S. Bresce, J. J. Sung, et al. Cluster of SARS Among Medical Students Exposed to Single Patient, Hong Kong. *Emerging infectious diseases*, 10(2):269, 2004.
 - [62] World Health Organization. *Pandemic Influenza Preparedness and Response: a WHO Guidance Document*. World Health Organization, 2009.
 - [63] K. Yadav, I. Kymmissis, and P. R. Kinget. A 4.4 μ W Wake-Up Receiver Using Ultrasonic Data. *IEEE Journal of Solid-State Circuits*, 48(3):649–660, 2013.
 - [64] E. Yoneki and J. Crowcroft. EpiMap: Towards Quantifying Contact Networks for Understanding Epidemiology in Developing Countries. *Ad Hoc Networks*, 2012.